

Synthesis and Structure of an Aluminophosphate Built from 3-Rings

David E. W. Vaughan,^{*,†} Hemant P. Yennawar,[‡] and Anthony J. Perrotta[†]

Materials Research Lab, Materials Research Institute, and Althouse Lab, Department of Biochemistry and Molecular Biology, Pennsylvania State University, University Park, Pennsylvania, 16802

Received September 26, 2005. Revised Manuscript Received June 8, 2006

By reacting a pre-made aluminophosphate (ALPO, P:Al = 0.9) gel with an aqueous tripropylamine solution of KOH and TMAOH, we have synthesized a new porous 3D crystalline structure (PSU-2) under high pH conditions. Single-crystal structure analysis shows that the orthorhombic crystal (*Pnna* with cell constants of $a = 12.741 \text{ \AA}$, $b = 10.2211 \text{ \AA}$, $c = 6.2239 \text{ \AA}$) is built from two different pairs of 3-rings of P tetrahedra and Al octahedra. Associated phases include ALPO analogues of the zeolites sodalite, analcime, and natrolite, the last not hitherto reported in an ALPO composition. The silicon-containing PSU-2 (SAPO) could not be made from an analogous SAPO gel.

Introduction

The discovery of aluminophosphate analogues of zeolites two decades ago¹ has greatly stimulated the interest in a wide variety of phosphates and substituted derivatives. The earlier neglected work of d'Yvoire² illustrated the potentially rich structural complexity of these materials, encompassing two- and three-dimensional frameworks and multiple coordinations of P and Al.³ Subsequent research has greatly expanded our structural and compositional knowledge.^{4,5} Our major interest is in using silicate and phosphate glasses and dried gels as slow-release nutrient sources for the growth of larger crystals. Most synthetic zeolites are made as submicrometer crystals suitable for catalytic, sorbent, and ion-exchange applications but are rarely large enough for conventional X-ray single-crystal structure analysis. Some success in growing large zeolite crystals has been achieved using several approaches, including nutrient gradients in gels,^{6–8} glass dissolution,⁹ use of organic solvents or solvent modifiers,^{10,11} and nucleation inhibition.¹² Compared to those of the silicate zeolites, ALPO compositions are particularly predisposed to crystallize large crystals, providing suitable substrates for the study of materials with nano- and subnanodimensional-

ity: nanotubes and rods, quantum dots, confined optically active molecules, etc.^{13,14} Our specific interest is focused on crystallizing large crystals using the lower reactivity of pre-made glasses and dried gels that have tailored aluminophosphate, gallophosphate, and silicate compositions with base metals and organic templates (primarily alkylammonium compounds and amines). In the case of the phosphates, such reactant sources seem to facilitate the crystallization of zeolitic phases at higher pH than previously reported.

Experimental Details

Synthesis Procedure. An aluminophosphate gel was prepared by first dissolving 363.7 g of $\text{Al}_2(\text{SO}_4)_3 \cdot 14\text{H}_2\text{O}$ (AlfaAesar) in 466 g of deionized water in a Hobart mixer followed by the slow addition of 179.2 g of H_3PO_4 (85%, EM Corp.). NH_4OH (29%, EM Corp.) was then slowly added until the pH reached 7.2. After mixing the solution for 25 min, with appropriate maintenance of the pH at 7.2 with NH_4OH addition, we vacuum-filtered the gel, washed it on the filter with 3 L of DI water, and dried it for 16 h at 100 °C. Weight loss after heating to 800 °C was 19.8%, and ICP-AES chemical analysis gave a P:Al of 0.91.

The above gel (2.15 g), ground and sieved to minus 40 mesh, was added to a solution of 2.4 g of KOH solution (45%, VWR), 6 g of DI water, 3.4 g of tetramethylammonium hydroxide solution (25%, SACHEM), and 1.3 g of tripropylamine (Fluka) in a 23 mL Parr Teflon-lined acid digestion bomb (pH 14). This represents a 1.29:0.56:1.1:1:0.91:70 $\text{K}_2\text{O}:\text{TMA}_2\text{O}:\text{TPA}:\text{Al}_2\text{O}_3:\text{P}_2\text{O}_5:\text{H}_2\text{O}$ reaction stoichiometry. After reaction for 260 h at 180 °C in an air oven, the crystalline product was filtered, washed with DI water, and dried at room temperature. Optical microscope evaluation indicated the presence of about 50% unreacted gel and at least two crystalline phases, one of which comprised faceted tabular orthorhombic crystals, up to 400 μm in the largest dimension, with unit prism, unit macrodome, brachypinacoid, and basal pinacoid. We have designated this product PSU-2. Partial separation of the products by sedimentation yielded a fine fraction mainly comprising crystals <2 μm and gel and a heavy fraction concentrated in the large PSU-2

* To whom correspondence should be addressed. E-mail: Dev4@psu.edu.

[†] Materials Research Institute, Pennsylvania State University.

[‡] Department of Biochemistry and Molecular Biology, Pennsylvania State University.

- (1) Wilson, S. T.; Lok, B. M.; Messina, A.; Cannan, T. R.; Flanigen, E. M. *J. Am. Chem. Soc.* **1982**, *104*, 1146.
- (2) d'Yvoire, F. *Bull. Soc. Chim. Fr.* **1961**, 1762.
- (3) Chen, J.-S.; Pang, W.-Q.; Xu, R.-R. *Top. Catal.* **1999**, *9*, 93.
- (4) Wilson, S. T. *Stud. Surf. Sci. Catal.* **2001**, *137*, 229.
- (5) Tuel, A.; Jorda, J.-L.; Gramlich, V.; Baerlocher, C. *J. Solid State Chem.* **2005**, *178*, 782.
- (6) Heinisch, H. K.; Dennis, J.; Hanoka, J. I. *J. Phys. Chem. Solids* **1965**, *26*, 493.
- (7) Ciric, J. *Science* **1967**, *155*, 291.
- (8) Charnell, J. F. *J. Cryst. Growth* **1971**, *8*, 291.
- (9) Shimizu, S.; Hamada, I. *Angew. Chem., Int. Ed.* **1999**, *38*, 2725.
- (10) Kuperman, A.; Nadimi, S.; Oliver, S.; Ozin, G. A.; Garces, J. M.; Olken, M. M. *Nature* **1993**, *365*, 239.
- (11) Ferchiche, S.; Valcheva-Traykova, M.; Vaughan, D. E. W.; Warzywoda, J.; Sacco, A., Jr. *J. Cryst. Growth* **2001**, *222*, 801.
- (12) Qui, S.; Yu, J.; Zhu, G.; Terasaki, O.; Nozue, Y.; Pang, W.; Xu, R. *Microporous Mesoporous Mater.* **1998**, *21*, 2450.

(13) Ozin, A. J. *Adv. Mater.* **1992**, *4*, 612.

(14) Behrens, P.; Stuckey, G. D. In *Comprehensive Supramolecular Chemistry*; Atwood, J. L., et al., Eds.; Pergamon: London, 1996; Vol. 7, p 721.

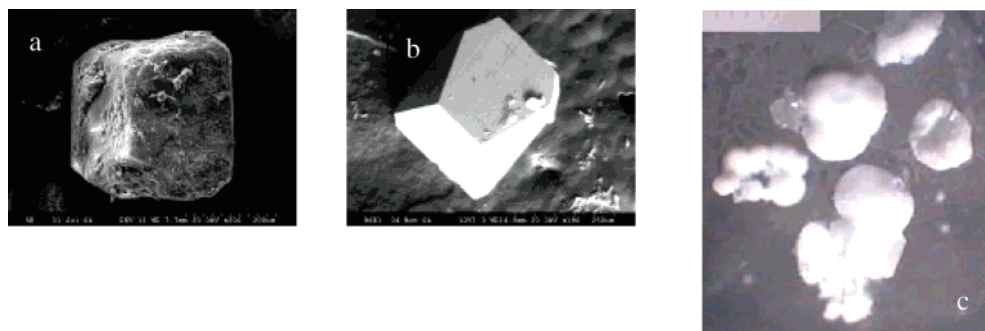


Figure 1. (a) PSU-2 coated with SOD and ANA microcrystals (0.45 mm \times 0.35 mm \times 0.25 mm); (b) clean PSU-2 from the 28 day experiment (scale same as that for part a); (c) “snowball” (NAT) phase with surface PSU-2 crystals (full scale = 0.1 mm).

orthorhombic crystals coated with microcrystals (Figure 1a). (The latter were readily cleaned off by rolling the large crystals on sticky tape.) The powder X-ray diffraction spectrum was complex, with ALPO—analcite (ANA) and ALPO—sodalite (SOD) identified as the microcrystalline phases and PSU-2 represented by the residual peaks. A repeat synthesis, aged for 28 days, yielded a larger fraction of the large PSU-2 crystals (up to 400 μ m in the largest dimension), hollow “snowballs” up to 500 μ m in diameter (Figure 1c) of radiating needlelike microcrystals, some with small PSU-2 crystals growing on their surface. Some of the snowballs were also growing on the facets of the PSU-2. These are tentatively identified as monoclinic ALPO—natrolite (NAT). This batch also included agglomerates of highly faceted PSU-2 crystals, a tight wall deposit on the Teflon vessel surface comprising <5 μ m crystals of ANA, in addition to microcrystalline SOD and unreacted gel. The snowball morphology is typical for the natural aluminosilicate mineral variety of NAT, called gonnardite.¹⁵

Increasing and decreasing the tripropylamine component ($\pm 50\%$) only marginally changed the relative amounts of the phases present. Similarly, replacing the ALPO gel with a similarly prepared SAPO gel in the first experiment had only a marginal effect on the product distribution: a minor morphology change on the PSU-2 (Figure 1b), but no silicon incorporation in the PSU-2 measured by microprobe analysis and no coating of microcrystals, the latter possibly indicating silicon incorporation into the ancillary phases. Repeating the first experiment at 150 $^{\circ}$ C produced no crystalline products. Calcination of PSU-2 at temperatures higher than 700 $^{\circ}$ C converts PSU-2 to a mixture of glass and an ALPO orthoclase phase shown in Figure 2.

Analytical Procedures. Samples were first evaluated using a stereo-optical microscope (20 \times to 90 \times) followed by powder X-ray diffraction using a Siemens D500 θ/θ powder diffractometer (Cu K α , Bragg–Brentano geometry, MDI Jade-6 software). In an attempt to separate multiple phases, we reslurried samples in 100 mL of DI water with a few drops of surfactant (DuPont Zeonyl FSA), transferred them to a 100 mL graduated cylinder, and decanted them in stages. The PSU-2 and snowball crystals were large enough to be hand-picked with the aid of the stereomicroscope. Photographic images (Figure 1) were obtained using a Leica DME optical microscope combined with a Javelin CCTV digital camera using Chromachip V software. The thermal stability of PSU-2 was evaluated using a Scintag-X2 X-ray powder diffractometer (15–35 $^{\circ}$ 2 θ , Cu K α) with a Pt strip heating attachment and sample platform. Thermogravimetric analyses (TGA) were run in air at a heating rate of 5 $^{\circ}$ C/minute using a TA Instruments 2960-SDT-V3 TGA/DSC unit. Scanning electron microscope (SEM) images and microprobe analyses were obtained using a Hitachi-3500S SEM. The aluminophosphate gel was analyzed by ICP-AES



Figure 2. TGA samples (top, transmitted light; bottom, reflected light; scale same as that as for Figure 1c) showing ex-solution glass globules on ALPO orthoclase pseudomorphs of PSU-2.

after fusion with lithium tetraborate (90%) and lithium carbonate (10%) followed by nitric acid dissolution.

Single-crystal structure analysis was done using a Bruker-AXS diffractometer using a fine-focused sealed tube with Mo K α radiation ($\lambda = 0.71073$ Å, 1600 W, 50 kV, 32 mA) and a CCD area detector at a distance of 5.8 cm. The crystal was clear, orthorhombic, and sized at 0.45 \times 0.30 \times 0.25 mm (shown in Figure 1a before removing surface microcrystals). A total of 1850 frames were collected with a scan width of 0.3 $^{\circ}$ in ω and an exposure time of 10 s/frame. The total data collection time was about 8 h. The frames were integrated with the Bruker SAINT software package using a narrow-frame integration algorithm. The integration of the data using an orthorhombic unit cell yielded a total of 6568 reflections in a θ angle range 3.20–28.01 $^{\circ}$ (0.90 Å resolution), of which 977 were independent, completeness = 99.3%, $R_{\text{int}} = 0.0221$, $R_{\text{sig}} = 0.0134$, and 971 were greater than $2\sigma(I)$. The final cell constants of $a = 12.741(2)$ Å, $b = 10.2211(16)$ Å, $c = 6.2239(10)$ Å, $\alpha = 90^{\circ}$, $\beta = 90^{\circ}$, $\gamma = 90^{\circ}$, $V = 810.5(2)$ Å³, are determined on the basis of the refinement of the XYZ centroids of 5924 reflections above $20\sigma(I)$ with $6.395^{\circ} < 2\theta < 56.011^{\circ}$. Analysis of the data showed negligible decay during data collection. Data were corrected for absorption effects using the multiscan technique (SADABS). The ratio of minimum to maximum apparent transmission was 0.847699.

Results and Discussion

PSU-2 Phase Analysis. Large PSU-2 crystals were hand-picked for single crystal and powder X-ray diffraction analysis. Crystals were ground and mounted as a film on a

(15) Tschernich, R. W. *Zeolites of the World*; Geoscience Press: Phoenix, AZ, 1992; p 217.

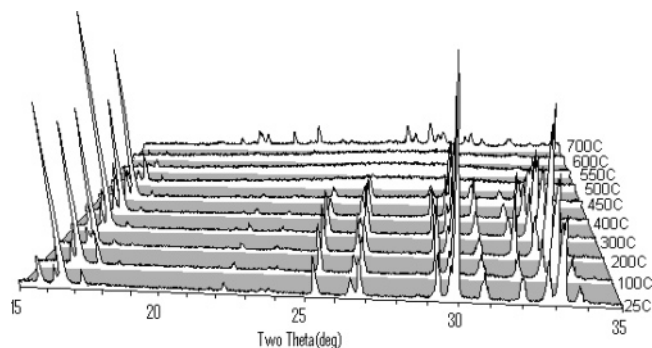


Figure 3. High-temperature powder XRD spectra showing PSU-2 destruction and recrystallization at temperatures higher than 500 °C.

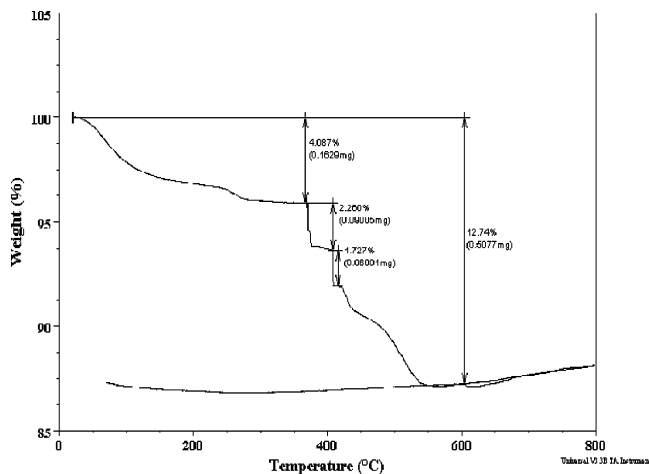


Figure 4. Thermogravimetric analysis showing the complex dehydration and dehydroxylation of the PSU-2 structure.

glass slide for X-ray powder diffraction analysis, but the pattern could not be matched with anything in our own zeolite/mineral database or the ICDD files. (A listing of the main diffraction peaks from 5–60° 2θ is given in the Supporting Information.) EDXRA microprobe analysis gave a composition 1:1.05:1 $K_2O:Al_2O_3:P_2O_5$ ratio, with no indication of an occluded carbon-containing template. Stepped calcination in a muffle furnace to 700 °C similarly showed no organic occlusion. The thermal stability of PSU-2 was evaluated using a Scintag-X2 diffractometer with a film of ground crystals of PSU-2 on the Pt strip heating attachment. The diffractograms were run after each 25 °C increment in temperature from 25 to 700 °C; for ease of viewing, only the 100 °C increments are shown in Figure 3. Decomposition occurs between 450 and 500 °C, forming an amorphous phase, followed by partial recrystallization between 600 and 700 °C to a phase analogous to orthoclase. A TGA experiment (Figure 4) showed gradual pore-water loss of 4 wt % up to 370 °C, followed by four smaller weight losses, including two sharp steps at 380 °C (2.3 wt %) and 410 °C (1.7 wt %), probably indicative of water loss from tight cage sites, and then two gradual steps (totaling 2.2 wt %). The final gradual weight loss of 2.5 wt % starts at 475 °C, the temperature at which the thermal XRD study shows structural degradation occurring, probably including final dehydroxylation of the framework. The DTA trace indicated structure decomposition starting at 430 °C (the start of the 2.2 wt % loss), melting at 510 °C, and recrystallization above 600 °C. Optical microscopy examination of the cooled samples from

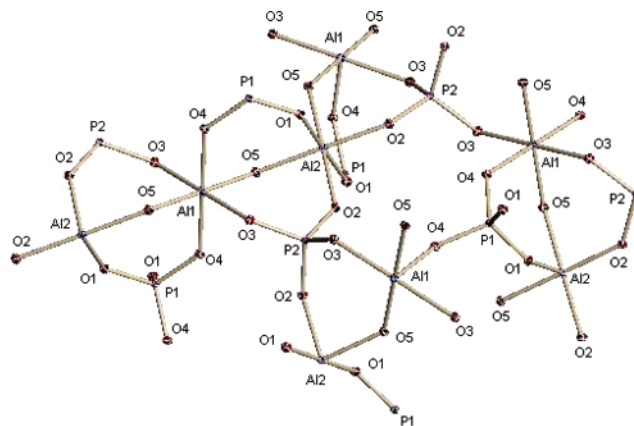


Figure 5. Structure projection tilted to show the connectivity of the two different pairs of connected 3-rings that constitute the building units of PSU-2.

Table 1. Atomic Coordinates and Equivalent Isotropic Atomic Displacement parameters (\AA^2) for PSU-2

	x/a	y/b	z/c	$U(\text{eq})$
K1	0.65176(4)	0.82248(5)	0.03795(8)	0.01348(16)
P1	0.43341(6)	0.7500	-0.2500	0.00445(18)
Al2	0.86744(7)	0.7500	-0.2500	0.0048(2)
Al1	0.5000	0.5000	0.0000	0.0050(2)
P2	0.7500	0.5000	-0.07060(12)	0.00430(18)
O3	0.65148(12)	0.52216(15)	0.0676(3)	0.0063(3)
O4	0.50791(12)	0.63470(14)	-0.2005(2)	0.0062(3)
O1	0.86541(12)	0.78133(15)	0.0543(2)	0.0064(3)
O2	0.76472(12)	0.62089(15)	-0.2160(2)	0.0063(3)
O5	0.47281(12)	0.61886(14)	0.2257(2)	0.0061(3)

both sets of thermal experiments confirmed that the samples had melted and partly recrystallized (Figure 2). On the basis of the microprobe and TGA data, the corrected composition, including water loss, is therefore about 2:1.05:1:2 $KOH:Al_2O_3:P_2O_5:H_2O$.

Single-Crystal Structure Analysis. The structure was solved and refined using the Bruker SHELXTL (version 6.1) software package using the space group $Pnna$ with $Z = 8$ for the formula unit $KAl PO_4(OH):0.30H_2O$. The final anisotropic full-matrix least-squares refinement on F^2 with 76 variables converged at $R1 = 2.61\%$, for the observed data and $wR2 = 7.39\%$ for all data. The goodness-of-fit was 1.238. The largest peak on the final difference map was $0.952 e^-/\text{\AA}^3$ and the largest hole was $-0.515 e^-/\text{\AA}^3$. On the basis of the final model, the calculated density was $2.902 g/cm^3$ and $F(000)$, $696 e^-$. Crystallographic details are summarized in Table 1.

Description of the PSU-2 Structure. The structure is built from two kinds of 3-ring pairs, each comprising two Al octahedra and one P tetrahedron. The first pair of nearly planar 3-rings shares an apical P tetrahedron, and the second pair, at nearly right angles, shares an edge comprising the two Al octahedra (Figure 5).

These connect to form a 3D structure with 6-rings parallel to the a and c axes; 4-rings of P tetrahedra cap opposite ends of a small cavity in the b axis, with a ring of eight Al octahedra circumscribing the enlarged cavity center. The basic unit is a chain of alternating Al octahedra and P tetrahedra linked through oxygens (Figure 6). Projections down the a , b , and c axes are shown in Figure 7. There are two possible potassium cation sites in the c axis channel,

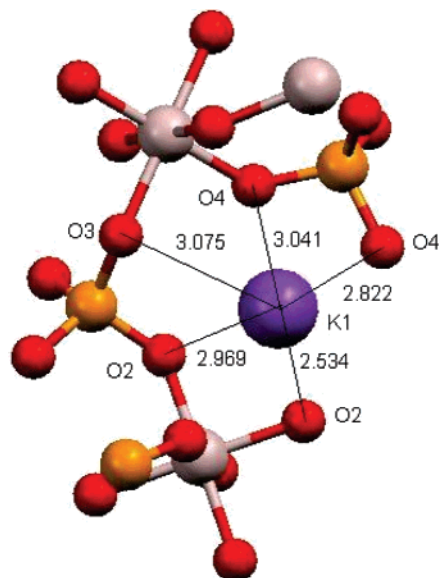


Figure 6. Chain of oxygen-linked, alternating Al octahedra and P tetrahedra forming the fundamental structural unit. The potassium cation position showing K–O bond lengths.

Table 2. Selected Interatomic Distances (Å) for PSU-2

K1–K1	3.0270(11)
K1–K1	3.8786(12)
P1–O4	1.5442(15)
P1–O1	1.5287(15)
P2–O3	1.5386(16)
P2–O2	1.5432(15)
Al2–O2	1.8705(16)
Al2–O5	1.9032(16)
Al2–O1	1.9209(15)
Al1–O5	1.8891(15)
Al1–O4	1.8610(15)
Al1–O3	1.9884(15)

but repeat refinements show K1 to have an occupancy factor of 95%. The connectivity of the two pairs of 3-rings is best illustrated in the projection shown in Figure 5. Views down the *a* and *c* axis channels show them to be formed by 6-rings of alternating P tetrahedra and Al octahedra connected by 3-rings comprising one P tetrahedron and two Al octahedra. The view down the *b* axis shows alternating 8-rings of Al-centered octahedra and 4-rings of P-centered tetrahedra. (Structures were drawn using Mercury software.¹⁶)

The P–O bond lengths (Table 2) vary between 1.529 and 1.544 Å; the octahedral Al–O distances vary between 1.86 and 1.99 Å, and O–P–O bond angles (Table 3) vary between 104.1 and 110.5°, all within the expected range. Although the protons of the hydroxyls could not be located by difference Fourier, it is likely that they are associated with the higher-temperature weight losses in the TGA and are on O5, the bridge between the Al-centered octahedra. These hydroxyls are not part of the phosphorus tetrahedra but, being weaker, they allow the formation of the three-membered rings comprising two connected Al octahedra and a P tetrahedron. However, there is not the expected increase in the Al–O5 distance. In ALPO-15,¹⁷ the Al–OH distances

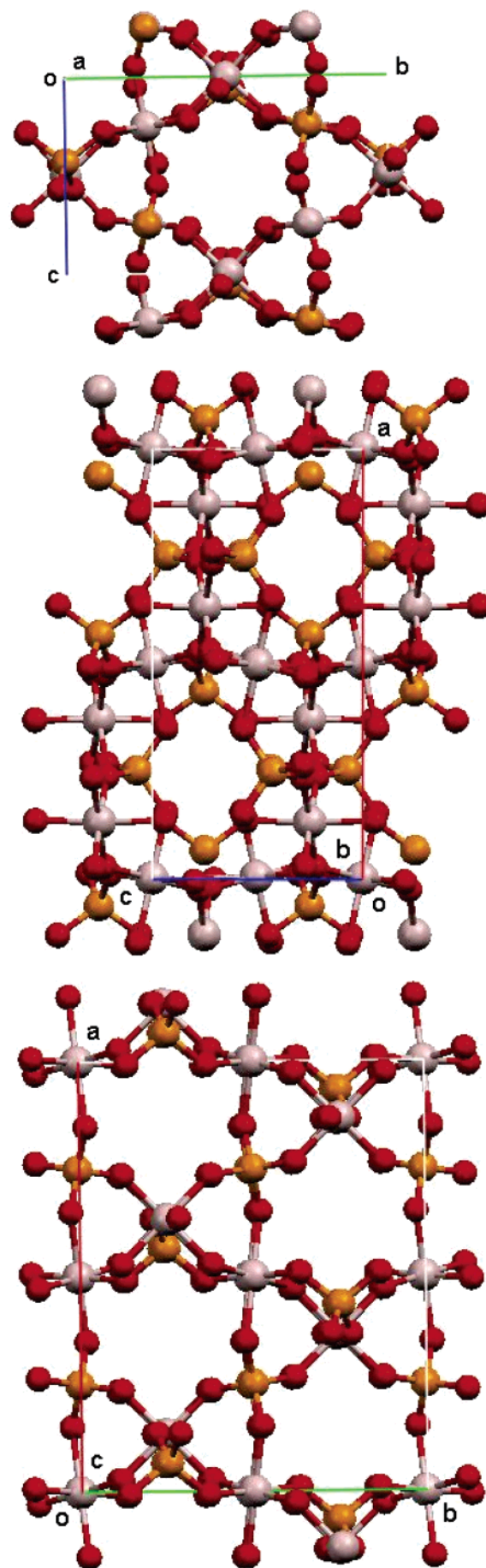


Figure 7. Projections of the structure down the *a* axis (top), *b* axis (middle), and *c* axis (bottom) showing unit-cell boundaries.

(16) Bruno, I. J.; Cole, J. C.; Edgington, P. R.; Kessler, M. K.; Macrae, C. F.; McCabe, P.; Pearson, J.; Taylor, R. *Acta Crystallogr., Sect. B* **2002**, *58*, 389.

(17) Pluth, J. J.; Smith, J. V.; Bennett, J. M.; Cohen, J. P. *Acta Crystallogr., Sect. C* **1984**, *40*, 2008.

Table 3. Selected Tetrahedral and Octahedral Bond Angles (deg) for PSU-2

O1#6-P1-O1#4	110.95(12)
O1#6-P1-O4	110.33(8)
O1#6-P1-O4#1	110.45(8)
O4-P1-O4#1	104.14(12)
O2-A12-O2#1	91.20(10)
O2-A12-O5#7	178.06(7)
O2-A12-O5#8	89.30(7)
O5#7-A12-O5#8	90.27(10)
O2#1-A12-O1#1	89.82(7)
O5#8-A12-O1#1	88.31(7)
O2#1-A12-O1	89.11(7)
O5#8-A12-O1	92.77(7)
O1#1-A12-O1	178.46(11)
O4#9-A11-O4	180.00(6)
O4#9-A11-O5	88.12(7)
O4#9-A11-O5#9	91.88(7)
O5-A11-O5#9	180.0
O4-A11-O3#9	89.71(6)
O5#9-A11-O3#9	86.98(6)
O4-A11-O3	90.29(6)
O5#9-A11-O3	93.02(6)
O3#9-A11-O3	180.0
O3-P2-O3#11	112.00(12)
O3-P2-O2#11	110.29(8)
O3-P2-O2	108.01(8)
O2#11-P2-O2	108.18(12)

are lengthened, whereas the more weakly bonded oxygen, part of a water molecule in an Al-centered octahedron, has a comparatively shorter interatomic distance of 1.94 Å. We have not been able to locate the water associated with the lower-temperature weight loss in the TGA, because it is not tightly bonded and is probably dispersed within the cavities of the structure. The O-Al-O apical bond angles vary between 178.1 and 178.5°, and the others are close to 90° (88.31–89.30°). Potassium cations occupy sites in the 6-rings of alternating P tetrahedra and Al octahedra with K-O bond distances between 2.53 and 2.92 Å. The K-K sites are 3.88 and 3.03 Å apart; the latter is shorter than the expected bond distance and is similar to a potassium-oxygen distance. This shorter-than-expected bond length suggests that this site is occupied, statistically, by both potassium and water, giving a chain of K-H₂O down the *c* axis. This is supported by repeat refinements, which give less than a fully occupied site for potassium (a 95% occupancy), which, when combined with an unusually large isotropic temperature factor for the potassium (much higher than those of the oxygens in the structure), indicates a partial occupancy of this site by potassium and water. (Reanalysis of four PSU-2 crystals (20 analyses) gave an average K:Al ratio of 0.91, confirming less-than-full K-site occupancy.)

Discussion

Because Brunner and Meier¹⁸ noted that the lowest framework density in zeolites is attainable with 3-ring structures, much interest has been focused on them. In the case of PSU-2, the framework density is high at 20 T atoms/1000 Å³ and is comparable to that of tridymite and cristobalite, which nonetheless may have a high capacity for small molecules.¹⁹ Although a dozen or more zeolites and like materials contain 3-ring secondary building units (sbu),

two are built from only 3-ring sbu's (NPO, RWY).²⁰ Although PSU-2 is not a zeolite in that it is built from octahedra and tetrahedra rather than only tetrahedra, it has zeolitic porosity. SBM-6 is a similar structure type built from only 3-rings of Al octahedra and P tetrahedra.²¹ It is interesting in that PSU-2 cocrystallizes with zeolitic ALPO SOD and ANA and a new ALPO composition for NAT. The TGA plot, after an initial pore-water loss, shows two sharp step weight losses between 375 and about 410 °C (exactly duplicated with the large crystals and a crushed sample) and the powder X-ray diffraction patterns remain essentially unchanged. This was confirmed with full single-crystal structure analysis on three large crystals heated in a muffle furnace at 425 °C for 30 min; two were transferred hot to a vial and stored over dried 3A molecular sieves to keep them "dry", and one crystal was fully equilibrated in moist air prior to mounting on the X-ray diffractometer. We ascribe these steps to the loss of water molecules from the cavity on the *b* axis, the separation into two steps possibly influenced by the relative proximity of the K cations to rings controlling egress of the water molecules. (Cation-controlled diffusion is a well-known phenomenon in zeolite LTA.) If these TGA steps were associated with dehydroxylation, there would be a symmetry change associated with the Al coordination going from six to four or five. The subsequent three weight losses in the TGA are also indicated as structural changes in the DTA, although only the final weight loss above 475 °C is correlated with a structural change in the thermal XRD study (Figure 3). The loss of structure above 475 °C with the further weight loss is indicative of dehydroxylation in these kinds of materials. The strong peaks in the weak X-ray diffraction pattern of the recrystallized material are typical for orthoclase, a potassium feldspar, in this case in the ALPO form. Pending work includes resolution of the PSU-2 complex thermal properties, including NMR studies, and a structure analysis of the snowball phase tentatively identified as having a monoclinic NAT structure similar to that of the mineral scolecite.

Acknowledgment. We thank Drs. Maria Klimkiewicz and Quigyi Lu for assistance in obtaining the SEM images and microprobe analyses and Nichole Wonderling for assistance with the high-temperature diffractometer. This work is supported by the Penn State Materials Research Institute and the Penn State MRSEC under NSF Grant DMR 0213623. We acknowledge NSF Grant CHE-0131112 for the purchase of a Bruker-AXS single-crystal X-ray diffractometer.

Supporting Information Available: A CIF file, a table of powder X-ray diffraction data for PSU-2, and complete tables of interatomic bond angles and bond lengths. This material is available free of charge via the Internet at <http://pubs.acs.org>.

CM0521572

- (19) Barrer, R. M.; Vaughan, D. E. W. *Trans. Faraday Soc.* **1967**, *63*, 2275.
 (20) Baerlocher, Ch.; Meier, W. M.; Olson, D. H. *Atlas of Zeolite Framework Types*, revised 5th ed.; Elsevier: Amsterdam, 2001; <http://www.iza-structures.org/databases/>.
 (21) Natarajan, S.; Gabriel, J.-C. P.; Cheetham, A. K. *Chem. Commun.* **1996**, 1415.

(18) Brunner, G. O.; Meier, W. M. *Nature* **1989**, *337*, 146.